Thermoanalytical and dilatometric studies of the Al_2O_3–Cu–Mo hybrid composite

J. Zygmuntowicz[1] · M. Piątek[2] · M. Wachowski[3] · P. Piotrkiewicz[1] · W. Kaszuwara[1]

Abstract

The present research is focused on the characterization of the composites from Al_2O_3–Cu–Mo system. The composites were prepared by slip casting method and subsequent sintering of green bodies in a reduced atmosphere. Two series of samples with different volume content of metallic powders were produced in the work: 10 vol% and 15 vol% of metal content with respect to the total solid-phase content. The sintering process of the composites was analyzed in detail. The linear shrinkage of the composites was measured. The shrinkage curves were obtained by dilatometry test in a heating mode. The composites were characterized by DTA/TG analyses and thermal conductivity. The composites were characterized by XRD, SEM, and EDX. The hardness was measured by Vickers hardness tester. Moreover, the Brazilian test was performed to determine the tensile mechanical properties of the composites. Fractography investigation was carried out as well. Dilatometric tests showed that the increase of the metallic phase volume in the ceramic matrix causes a decrease in the starting temperature of densification. Simultaneously, dilatometric experiments indicated that an increasing amount of metallic particles into the ceramic matrix increases the temperature of maximum densification and decreases the total shrinkage of the composites during sintering. The DTA/TG showed the characteristics of the dispersant decomposition to the atmosphere during thermal treatment and increase of mass connected with the oxidation of metals. Fractography results revealed good adhesion between Al_2O_3 matrix and the metallic phase. The observation allowed to conclude that the Al_2O_3 matrix surface is characterized by the brittle fracture mechanism.

Keywords DTA/TG analyses · Dilatometry test · Thermal conductivity · Slip casting · Ceramic–metal composite

Introduction

The current literature knowledge indicates that hybrid composites can be obtained using a variety of methods. The most popular techniques for obtaining ceramic–metal composites are as follows: slip casting [1], hot pressing [2], electro-discharge compaction (EDC) [3], field-assisted sintering technique (FAST) [4], spark plasma sintering (SPS) [5, 6], and pulse plasma compaction (PPC) [7]. The Al_2O_3–Cu composite reveals high strength, high electric, and thermal conductivity with additional high wear resistance. Microstructure and mechanical properties of Al_2O_3–Cu composite are described well in literature [8]. Oh et al. [9] investigated two types of fabrication methods and its influence on mechanical properties and microstructure of Al_2O_3–Cu composites. Pietrzak et al. [10] revealed that during sintering process, the layer of spinel crystallites is formed on the Al_2O_3–Cu boundary, and own research shown that slip casting technique allows to production of Al_2O_3–Cu composite without spinel crystallites [11]. The slip casting method is a highly efficient technique used to produce ceramic–metal composites. Problem in production of this type of composite is melting and flowing of copper phase during the casting process. This is due to high differences in temperature of sintering of Al_2O_3 and temperature of copper

✉ J. Zygmuntowicz
  zygmuntowicz.justyna@pw.edu.pl

1 Faculty of Materials Science and Engineering, Warsaw University of Technology, 141 Woloska St., 02-507 Warsaw, Poland

2 Research Laboratory, Łukasiewicz Research Network, Institute of Ceramics and Building Materials, Ceramic and Concrete Division in Warsaw, 9 Postepu St., 02-676 Warsaw, Poland

3 Faculty of Mechanical Engineering, Military University of Technology, gen. W. Kaliskiego 2 Str., 00-908 Warsaw, Poland

melting. In this case, optimization of the production process is highly required. The proposition of the solution to this problem is adding the second metallic phase in which temperature of melting is much higher than the temperature of copper melting. The suitable metal which fulfils this requirement and can be used as an additional phase in the hybrid composite is molybdenum. In literature exists information about composites with molybdenum used as a metallic phase [12]. As well, Al_2O_3–Mo composite is described well [13]. Chmielewski et al. [2] revealed experimental procedure to obtain Al_2O_3–Mo characterized by high density and very stable bonding between ceramic and metal phase. Nawa et al. [14] revealed that fracture toughness of Al_2O_3 with 20 vol% Mo fabricated by the hot-pressed composite is 1.8 times larger than the samples consisted of monolithic Al_2O_3. This research may suggest that the addition of molybdenum particles improves the mechanical properties of samples without metallic particles in case samples manufactured by the hot-pressed. Additionally, results of Sbaizero et al. [15] research indicated that 20 vol% of molybdenum in Al_2O_3–Mo composites is a minimum to obtain an effective increase of toughness.

Therefore, the addition of molybdenum may ameliorate the wettability of the metal phase during the fabrication of these type composites. As a consequence, it can cause prevent liquid copper from leaking from the composite during the sintering process. Moreover, due to the proposed Al_2O_3–Cu–Mo is a novel hybrid ceramic–metal composite, it is important to investigate the relationship between the slip casting process parameters, composite structure, and mechanical properties concerning the content of metallic phases. Therefore, in this paper research on Al_2O_3–Cu–Mo fabricated by the slip casting method with different content of Cu and Mo phases is presented. Obtained research results would be useful to increase knowledge about hybrid composites from alumina–metallic phases system. Moreover, a meticulous study of the selected properties of fabricated composite materials seems to be greatly helpful from an application point of view. Such materials due to the type of components used to manufacture them can be used as elements of sensors. The properties of Al_2O_3–Cu–Mo composites enable potential high-technology applications as structural materials.

Experimental

The experiments were performed on commercially available powders. The composites were fabricated from an α-Al_2O_3 powder (TM-DAR, Taimei Chemicals) of a purity of 99.99% and an average particle size of 0.145 μm, specific surface area 10.85 $m^2 g^{-1}$, and density of 3.98 g cm^{-3}; a Cu powder (Createc, Poland) with an average particle size of 99.53 μm, specific surface area 0.09 $m^2 g^{-1}$, and density of 8.96 g cm^{-3}; and a Mo powder (Createc, Poland) with an average particle size of 8.5 μm, specific surface area 0.24 $m^2 g^{-1}$, and density of 10.28 g cm^{-3}. The properties of the raw materials are shown in Table 1. The densities of the powders were determined by a helium pycnometer, AccuPyc 1340 II (Micromeritics), in a sequence of 100 purges and 100 measurement cycles. The SEM micrographs and X-ray diffraction patterns of the starting material particle of metal powders are shown in Fig. 1. It was found that molybdenum powder (Fig. 1a) was characterized by a regular surface close to spherical in contrast to copper powder (Fig. 1b) which is distinguished by a highly irregular surface with numerous cavities.

Two series of composites were prepared by slip casting: Series I—Al_2O_3 + 10 vol% of the metallic phase (Cu + Mo) and Series II—Al_2O_3 + 15 vol% of the metallic phase (Cu + Mo), respectively. In the present study, slurry with 50 vol% of solid content was obtained. The volume of metal was calculated with respect to the total metal volume content in the suspensions. In both series, the ratio of metals in suspensions was in the same proportions of 50 vol% by Cu to 50 vol% by Mo. In the research, deionized Milli-Q water was applied as the solvent. Duramax D3005 was applied as the dispersant in the suspensions. The Duramax-D3005 substance is the ammonium salt of a polyelectrolyte useful for dispersing a variety of ceramic/metal and ceramic powders in demineralized water [16, 17]. The slurry included 1.5 mass% of the dispersant with respect to the total solid content mass in all samples.

The stability of the slurry during the prepared samples by the slip casting method is very important. Therefore, macroscopic observation of two slurries with 50 vol% of solid content with different metal content (10 vol% and

Table 1 Properties of the raw materials

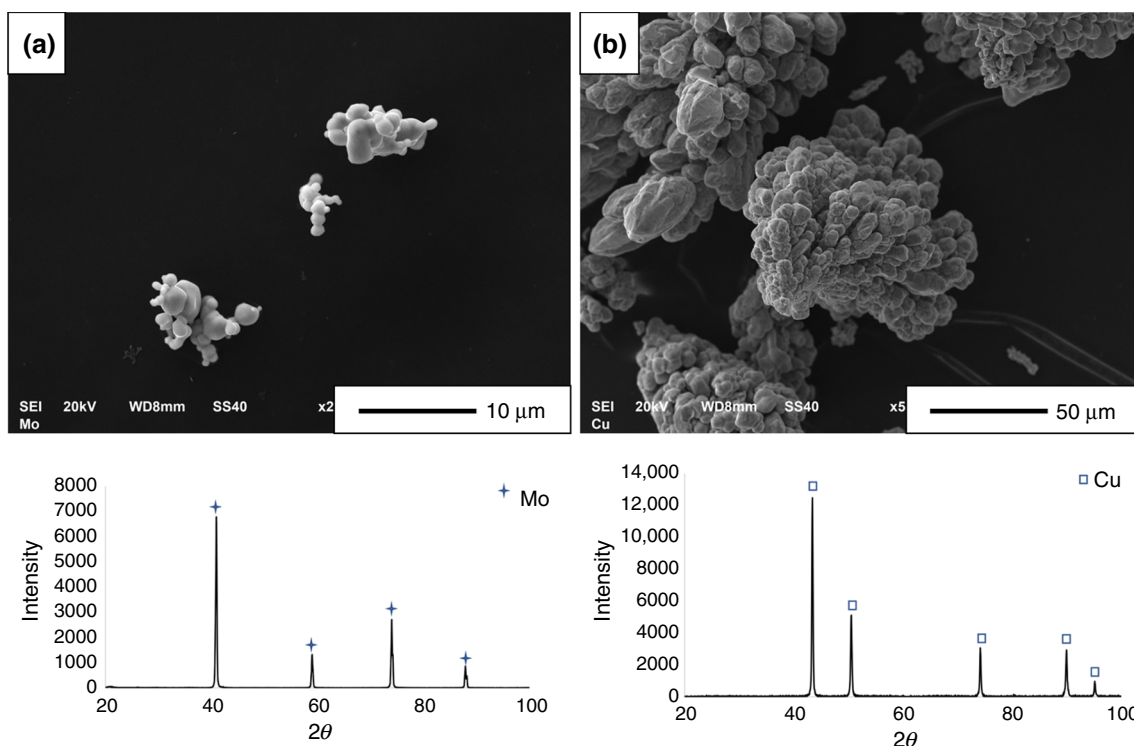| Properties	Mean particle size from SEM investigation/μm	Density from helium pycnometer/g cm^{-3}	Specific surface area/ $m^2 g^{-1}$	Melting point/°C	Modulus of elasticity/ GPa
α-Al_2O_3	0.145 ± 0.055	3.98	10.85 ± 0.07	2072	370
Cu	99.53 ± 23	8.96	0.09 ± 0.01	1085	110
Mo	8.5 ± 1.2	10.28	0.24 ± 0.01	2610	330

Fig. 1 SEM images and XRD patterns of the starting metal powders: **a** Mo, **b** Cu

15 vol%) during the sedimentation test was made. Suspension samples with volumes of 5 mL and various concentrations were poured into individual test tubes. The experimental time was 48 h. The sedimentation test was conducted at room temperature (25 °C), and images were gained with a digital camera every 2 h.

In this work, the samples were prepared in several steps. In the beginning, Duramax-D3005 and subsequently the copper and molybdenum metal powders and alumina powder were added to the deionized water. The prepared slurry was ball-milled for 1.5 h with 300 rpm for good homogenization. In the sequent step, the suspensions were degassed in a device for automatic slurry mixing and degassing (ARE-250 fabricated by Thinky Corporation) for 5 min at the rate of 1800 rpm. This device allows releasing bubbles smaller than 1 μm from the prepared suspensions. The optimal parameters of the process were first established based on a set of trials. Subsequently, the prepared slurry was poured into a gypsum mold. Thanks to the use of porous molds, the water from the slurry was absorbed by the gypsum mold, and a green cast was obtained. Thereafter, the gypsum mold with the sample inside was dried in a vacuum chamber for 24 h at 40 °C. Then, the dried and shrunk composite was removed from the gypsum mold. During the last step, the samples were sintered at 1400 °C for 2 h in nitrogen atmosphere.

DTA/TG/DTG measurements have been performed for the two series of Al$_2$O$_3$ samples with different metal content 10 vol% of the Cu + Mo (Series I) and 15 vol% of the Cu + Mo (Series II) in nitrogen atmosphere. The TG/DSC measurements were carried out by using a STA 449 Jupiter F1 instrument (Netzsch, Germany). The heating rate was 40 °C min^{-1}, and the final temperature was 1500 °C. The green samples were shredded to obtaining powder form, and after that, the mass of the sample was determined (sample mass ~ 30 mg) and put in the corundum Al$_2$O$_3$ crucible to test its thermal behavior.

The linear shrinkage was determined by dilatometer DIL 402 E (Netzsch, Germany). Composite samples were shaped into cylindrical rod. The dimensions of the specimens were 6 mm in diameter and 14 mm in length, the transversal external surfaces being polished to guarantee plan parallel surfaces for precise positioning within the measuring head. The samples were heated up to 1400 °C with constant heating rate of 10 °C min^{-1}, in helium atmosphere and in a furnace with graphite heating elements. Due to the specific design of the device, the measurements are carried out in a helium atmosphere, because it is chemically inert and there are no technical safety restrictions in the use of this gas. Prior measurement, calibration was carried out with graphite standard of the known properties and expansion. The measurement (correction measurement and also measurement of the green samples of the Al$_2$O$_3$–Cu–Mo hybrid composite) was carried out under the same conditions (temperature heating program, atmosphere, gas flow rate) in

order to determine the signals related to the expansion of the device elements and to correct the results obtained during the proper measurement.

The determination of the change in linear dimension during shrinkage makes it possible to establish the necessary technical parameters like the commencement and termination of the sintering of the ceramic and composites bodies which afford an indirect assessment of the sintering kinetics.

Thermal diffusivity of the sintered samples was measured by the laser flash method using LFA 427 instrument (Netzsch, Germany), at the temperature range of 25–700 °C. The measurements were performed in argon, using samples with a diameter of 3 mm in diameter and a thickness of 3 mm. The construction of the apparatus allows for measurements in an inert gas atmosphere of high purity, and argon is safety for sample and furnace chamber. Before conducting the experiments, the surfaces of samples were covered by thin layer of graphite. In carrying out a measurement, the lower surface of a plane parallel sample is first heated by a short energy pulse. The resulting temperature change on the upper surface of the sample is then measured with an infrared detector. The direct effect of the measurement is to determine the thermal diffusivity coefficient or temperature uniformity coefficient, which is obtained based on the analysis of changes in the surface temperature of the sample not illuminated by the laser beam. The recorded changes in the temperature of the material are the result of the absorption of the laser pulse through the head of the material of the test sample.

Thermal diffusivity is determined with the use of the Eq. (1) given by Parker et al. [18]:

$$\alpha = \frac{0.1388 \cdot L^2}{t_{0.5}} \tag{1}$$

where $t_{0.5}$ is the time required for back surface temperature rise to reach half of its maximum, and L is a sample thickness.

Thermal conductivity was calculated based on the following formula (2) [19]:

$$\lambda = \alpha \cdot \rho \cdot C_p \tag{2}$$

where λ—thermal conductivity, α—thermal diffusivity, ρ—density of the measured sample, C_p—specific heat of the material.

These results represent the average value of four independent tests at individual temperatures.

The specific heat capacity of the Al_2O_3 sample and Al_2O_3 composite with addition of the metallic particles was determined by using differential scanning calorimetry DSC 204 F1 Phoenix® (Netzsch, Germany). In first stage, the measurement with two empty samples was taken to obtain a baseline. In next step, the reference curve was obtained by using

a pan containing sapphire standard disk and an empty pan, and the measurement on a pan containing sample and an empty pan was carried out. The heating was performed at temperature of 20–500 °C with 10 °C min⁻¹ heating rate in nitrogen atmosphere.

These results represent the average value of four independent tests at individual temperatures. The specific heat of the measurement samples was determined by comparison with graphite standard of known specific heat.

The XRD study was carried out to identify bulk crystalline phases of the samples. The Rigaku MiniFlex II diffractometer with CuK_α ($\lambda = 1.54178$ Å) is used for X-ray diffraction analysis. The X-ray measurements were carried out at room temperature. The spectra were scanned at a rate of 1 deg min⁻¹ in the range $2\theta = 10°–100°$. The analyses were done at the cross section of composites.

The density of the sintered composites was measured by the Archimedes technique using distilled water as the buoyant medium. The measurements were made for 25 samples in each series.

The microstructures of the cross-sectional samples were characterized using a JSM-6610 scanning electron microscope (SEM) operated at 10–15 kV. Before observations, samples were carbon-coated using Quorum Q150T ESS coating system. SEM was used for fractography investigation as well. The chemical compositions were characterized by using energy-dispersive X-ray spectroscopy detector. EDX chemical composition analysis of the samples was done at acceleration voltage 15 kV. The cross sections were made by cutting the samples along the axial direction with a diamond saw. The polished cross sections were done by grinding and polishing with 1 μm diamond paste and silica suspension.

Furthermore, the hardness was measured on a Vickers hardness tester (WPM LEIPZIG HPO-250) for sintered and polished samples. The hardness was determined by used means of a Vickers indenter with a load of 196 N with 15 s holding time.

The Brazilian test was performed to determine the tensile mechanical properties of the composites. The Brazilian test was accomplished according to ASTM standard [20]. The foundations on which the Brazilian test is based are that the samples are isotropic and uniform, and it behaves elastically. Moreover, samples show shear and compression strengths greater rather than the tensile strength [21]. The tensile stress can be calculated from the following Eq. (3) [20, 22–24]:

$$\sigma = \frac{(2 \cdot F)}{(\pi \cdot D \cdot t)} \tag{3}$$

where F is the load applied on the composites, and D and t are, respectively, diameter and thickness of the samples.

Results and discussion

Figure 2 shows the collected photographs during the sedimentation test. During the investigation time, no sedimentation was observed in both suspensions (Fig. 2). It was shown that even after 24 h, both slurries were stable and any phase separation was not noticed. The obtained result indicated that particles disperse well in suspensions.

Thermal analysis is a very useful tool to determine decomposition stages of different organic and inorganic substances, that is, to observe the behavior of materials as a function of increasing temperature. DTA, TG, and DTG

curves for the Al₂O₃ composites with addition of 10 vol% (Series I) and 15 vol% (Series II) of the metallic phase into nitrogen are shown in Fig. 3.

Figure 3 presents DTA/TG/DTG curves of Al₂O₃–Cu–Mo green body in which the concentration of the metallic phase was 10 vol% and 15 vol%. In range of temperatures from 30 to 600 °C, the small but so wide exothermic peaks on DTA curve with the maximum at 299 °C and 426 °C for the Al₂O₃ composites with addition of 10 vol% and 296 °C and 440 °C for the Al₂O₃ composites with addition of 15 vol% are visible. Based on the obtained results, it can be concluded that these peaks correspond with the mass loss indicates on the thermal decomposition of the Duramax D3005,
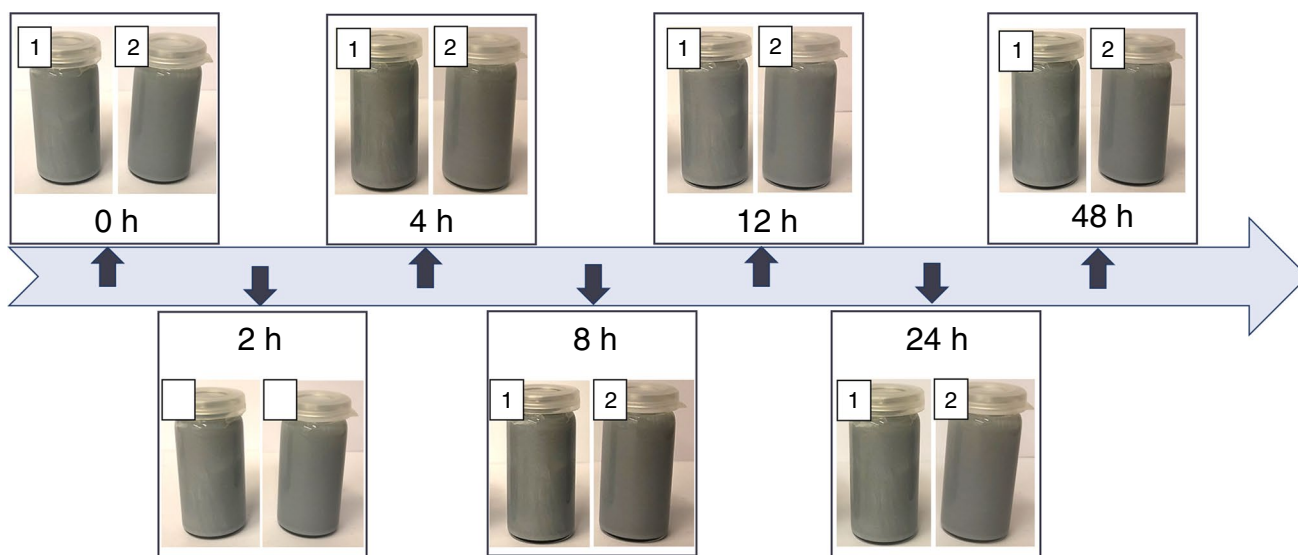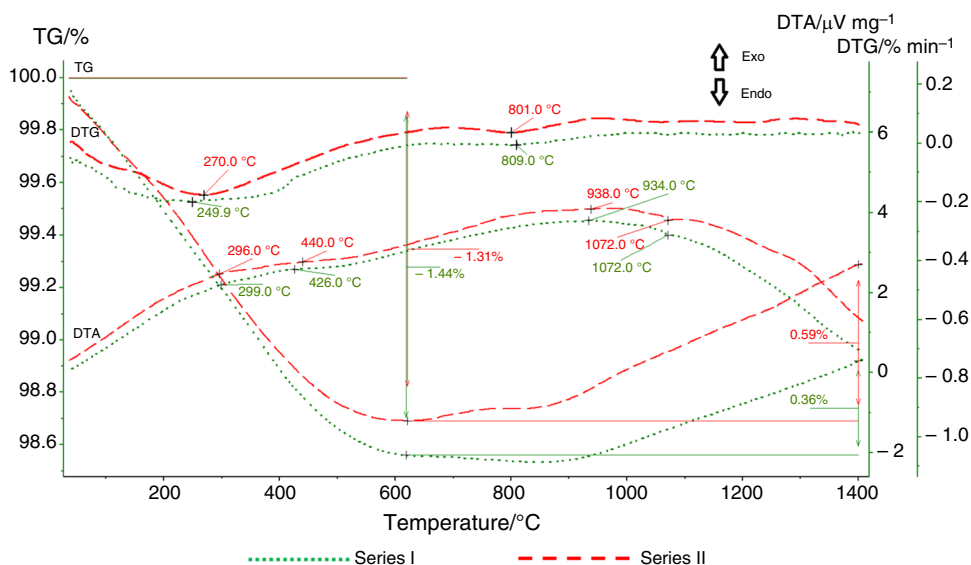

Fig. 2 Sedimentation test for slurry with 50 vol% of solid content where: 1—suspensions with 10 vol% of the metal particles and 2—suspensions with 15 vol% of the metal particles with respect to the total solid-phase content

Fig. 3 DTA/TG/DTG curves of Al₂O₃ composites with addition of 10 vol% and 15 vol% of the metallic phase (Cu + Mo)

which was used as a dispersant in the suspension. Total mass loss observed until ca. 600 °C (~ 1.44% for samples with 10 vol% of the metallic phase and 1.31% for samples with 10 vol% of the metallic phase) confirms the fact that the slurry from which the samples were prepared included 1.5 mass% of the dispersant. Based on literature reports [25], it can be concluded that the peaks on DTA curves in range from 30 to 600 °C can be ascribed to thermal decomposition of the acrylic homopolymer toward H_2O and CO_2. Above the temperature of 600 °C, the increase in mass is observed till 1400 °C, which can be ascribed to the oxidation of Cu and Mo. The mass increase in the temperature range 600–1400 °C equaled to 0.36% in the case of Al_2O_3 composites with addition of 10 vol% of the metallic phase (Series I) and about 0.59% for composites with 15 vol% (Series II). The difference in the mass increase of the samples is related to the amount of metallic phase in the test sample. Higher content of the metallic phase in the samples leads to higher growth of mass. On DTA curves, at 1072 °C (for both samples) endothermic peaks are visible. These peaks are associated with molybdenum melting.

Linear shrinkages and linear shrinkage rates for the green samples after dilatometric experiments are shown in Fig. 4. Linear shrinkage rates facilitate the study of the sintering kinetics associated with the densification process of the aluminum oxide. The sintering behavior is clearly related to the additive composition investigated and the amount of this composition. Total shrinkage of samples, temperature of densification start, and temperature of maximum densification for individual samples are summarized in Table 2. Dilatometric measurements showed that the addition of Cu and Mo particles into Al_2O_3 matrix shifted starting densification temperature toward a higher temperature, in comparison with the pure Al_2O_3 sample. Dilatometric tests showed that the addition of Cu + Mo particles into Al_2O_3 matrix

Table 2 Total shrinkage of samples, starting densification temperature, and temperature of maximal densification for individual samples, where T_{sd}—starting densification temperature; T_{md}—temperature of maximal densification

Samples	T_{sd}/°C	T_{md}/°C	Shrinkage/%
Al_2O_3	1097.7	1276.9	14.29
Series I— Al_2O_3 + 10 vol% metallic phase (Cu + Mo)	1209.2	1325.0	9.89
Series II— Al_2O_3 + 15 vol% metallic phase (Cu + Mo)	1205.0	1342.1	8.38

shifted starting densification temperature for ~ 111 °C in the case of the composite with 10 vol% of the metallic phase and ~ 107 °C when 15 vol% of the metallic phase was added, in comparison with the pure Al_2O_3 sample. However, it can be seen that the starting densification temperature for sample with higher addition of the metallic phase moves to lower temperatures. The maximum densification rate for the pure Al_2O_3 samples is at about 1276 °C, whereas this temperature is increased to 1325 °C and 1342 °C for the composites with 10 vol% (Series I) and 15 vol% (Series II) of metallic phase, respectively. The experimental results indicate that total shrinkage of the pure Al_2O_3 sample reached ~ 14% at 1400 °C. Therefore, dilatometric experiments confirmed that 10 vol% and 15 vol% Cu and Mo particles addition leads to the decrease of the total shrinkage at 1400 °C to 9.89% and 8.38%, respectively. Thus, the addition of more metallic particles in the alumina matrix causes lowering of the starting densification temperature, an increase of the temperature where the maximum densification rate occurs, and the decrease of the total shrinkage.

Fig. 4 Linear shrinkage and linear shrinkage rate curves of Al_2O_3 sample and Al_2O_3 composites with addition of 10 vol% and 15 vol% of the metallic phase (Cu + Mo) as a function of temperature
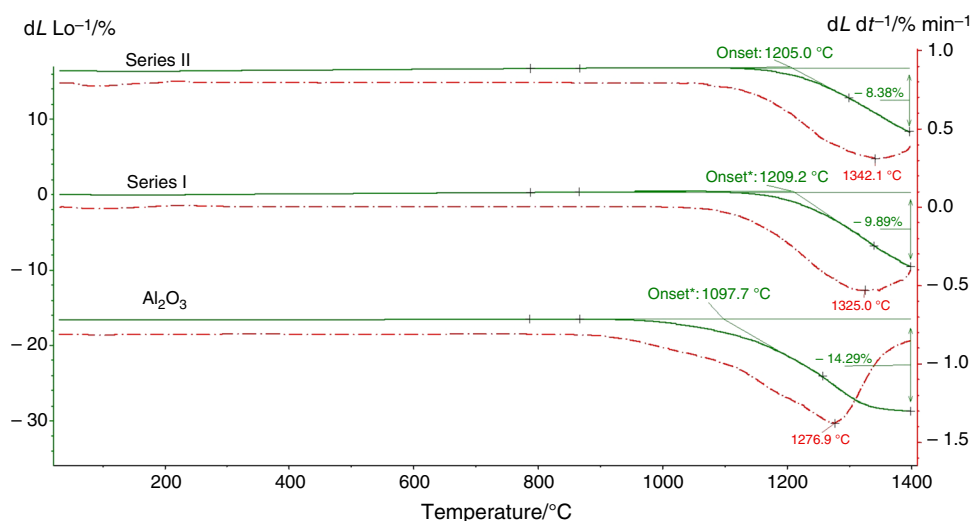
Thermal conductivity, thermal diffusivity, and specific heat capacity are the most important thermophysical material parameters for characterizing the thermal transport properties of a material or component. Figures 5 and 6 shows the thermal diffusivity, specific heat capacity, and thermal conductivity of the prepared samples.

As can be seen in Fig. 5, specific heat capacity of Al_2O_3 composites decreased when the volume of the metallic phase increased. However, specific heat capacity of all measured samples, regardless of the presence of Cu and Mo particles, increased with increasing temperature.

Similarly, as in the case of specific heat capacity, the diffusivity decreases with increasing temperature. In temperature from 25 to 50 °C, the samples from pure Al_2O_3 are characterized by the highest values of the thermal diffusivity (Fig. 6). The experimental results indicate that above the temperature of 100 °C, the diffusivity of the Al_2O_3 composites with the addition of the metallic phase increases, over the diffusivity of the sample from Al_2O_3. Up to 400 °C, samples with the addition of 15 vol% of the metallic phase are characterized by the highest diffusivity, while above this temperature samples with the addition of 10 vol% of the metallic phase.

Based on measurement results, it was found that the course of the thermal conductivity curve for the Al_2O_3 sample, as well as the samples with addition of the 10 vol% (Series I) and 15 vol% (Series II) of the metallic phase, is similar, and the conductivity decreases with increasing temperature. The studies of thermal conductivity indicate that at 25 °C the highest value of thermal conductivity, the sample of aluminum oxide is characterized, which is equal to ~28 W m K^{-1} (Fig. 7). It should be noted that in higher temperatures, above the temperature of 50 °C, increase in the thermal conductivity of the samples with the addition of the metallic phase was observed. The results obtained in
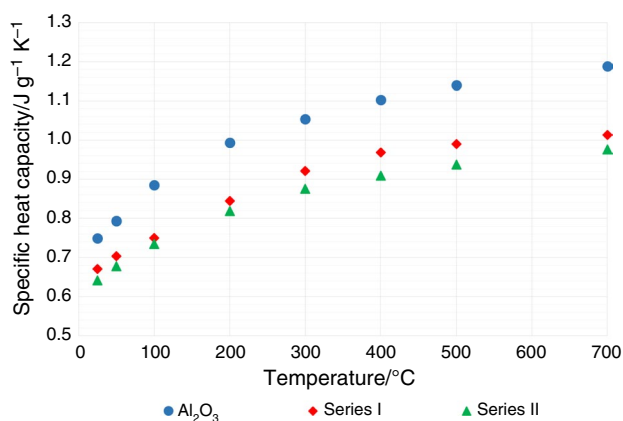

Fig. 6 Thermal diffusivity and specific heat capacity for the Al_2O_3 sample and also for the Al_2O_3 matrix with addition of 10 vol% (Series I) and 15 vol% (Series II) of the metallic phase as a function of temperature
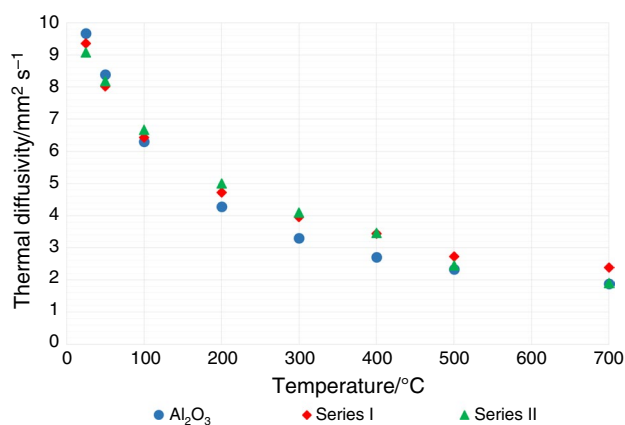
this study indicated that the thermal conductivities of Al_2O_3 composites decreased with increasing Al_2O_3 percent. This was attributed to the thermal conductivity of Al_2O_3 which is lower so far of copper and molybdenum thermal conductivity. The decrease of the thermal conductivity of the samples with the addition of 15 vol% of the metallic phase, in higher temperatures, can be associated with inhomogeneous distribution of the metal particles in the sample volume. The second reason is the agglomeration of some metal particles at the grain boundaries which can form a kind of grain boundary phase that increases the scattering of the charge carrier, hence reducing the thermal conductivity.

Figure 8 shows the XRD patterns of the samples of each series after sintering. It was found that in the case of both series, the observed peaks indicate the presence of alumina, copper, and molybdenum phases. The measurements
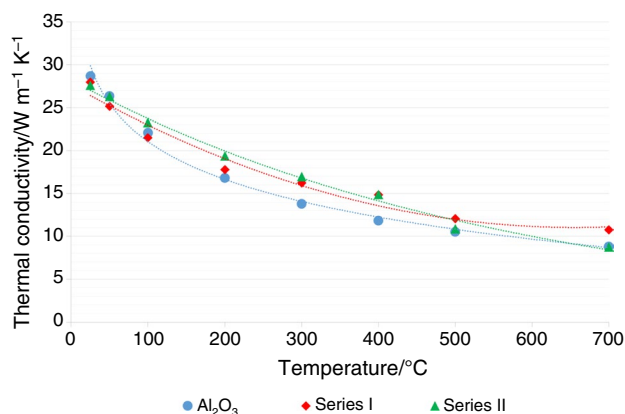

Fig. 5 Specific heat capacity for the Al_2O_3 sample and also for the Al_2O_3 matrix with addition of 10 vol% (Series I) and 15 vol% (Series II) of the metallic phase as a function of temperature

Fig. 7 Thermal conductivity for the Al_2O_3 sample and also for the Al_2O_3 matrix with addition of 10 vol% (Series I) and 15 vol% (Series II) of the metallic phase as a function of temperature

Fig. 8 X-ray diffraction analysis of the specimens: **a** Series I—$Al_2O_3 + 10$ vol% of the metallic phase (Cu + Mo) and **b** Series II—$Al_2O_3 + 15$ vol% of the metallic phase (Cu + Mo)
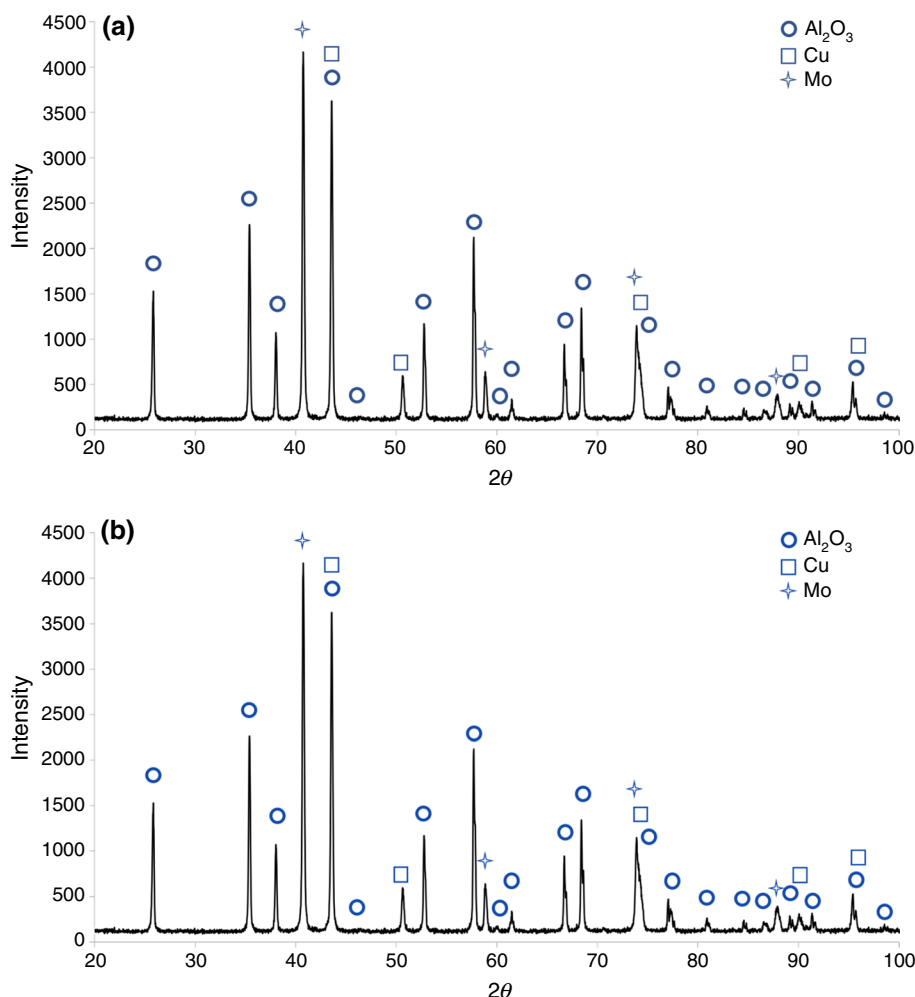
allowed to observe that after the sintering process, no new phase has been established. The use of a nitrogen atmosphere prevents the oxidation of the metal and created new phases during sintering.

The selected properties of the prepared composites are presented in Table 3. The measurement showed that the relative density of the sintered composites is similar for both series. The relative density equal to the level 98% in both series may mean that the formed composites are described by a high degree of packing of the grains in the sintered samples. A slight decrease in the value of volume shrinkage for the Series II compared to Series I was noted. Increasing the metallic phase in the composite resulted in

a decreasing in volume shrinkage. The open porosity for both series was determined to be less than 1%.

A typical microstructure of samples after sintering is shown in Fig. 9. The dark areas on the micrograph correspond to the ceramic matrix, while the bright areas are the metallic phase. The Al_2O_3–Cu–Mo composite consists of the two metal phases: light gray and semi-dark gray phase, and according to the results of XRD analysis, they are Mo and Cu, respectively. It can be seen from Fig. 9a, b that, the sintered composites have a compact structure without obvious holes, cracks, and other defects on their surface. The scanning electron microscopy research has revealed the not homogeneous distribution of the metallic phase in prepared composites. It was observed

Table 3 The selected physical properties of composites

Selected physical property of composites	Relative density/%	Volume shrinkage/%	Open porosity/%
Series I—$Al_2O_3 + 10$ vol% metallic phase (Cu + Mo)	98.46 ± 1.24	35.23 ± 0.83	0.84 ± 0.73
Series II—$Al_2O_3 + 15$ vol% metallic phase (Cu + Mo)	98.47 ± 1.53	33.56 ± 0.94	0.79 ± 0.64

Fig. 9 SEM micrographs of cross section of Al$_2$O$_3$–Cu–Mo composite obtained by slip casting: **a** Series I—Al$_2$O$_3$ + 10 vol% of the metallic phase (Cu + Mo) and **b** Series II—Al$_2$O$_3$ + 15 vol% of the metallic phase (Cu + Mo)
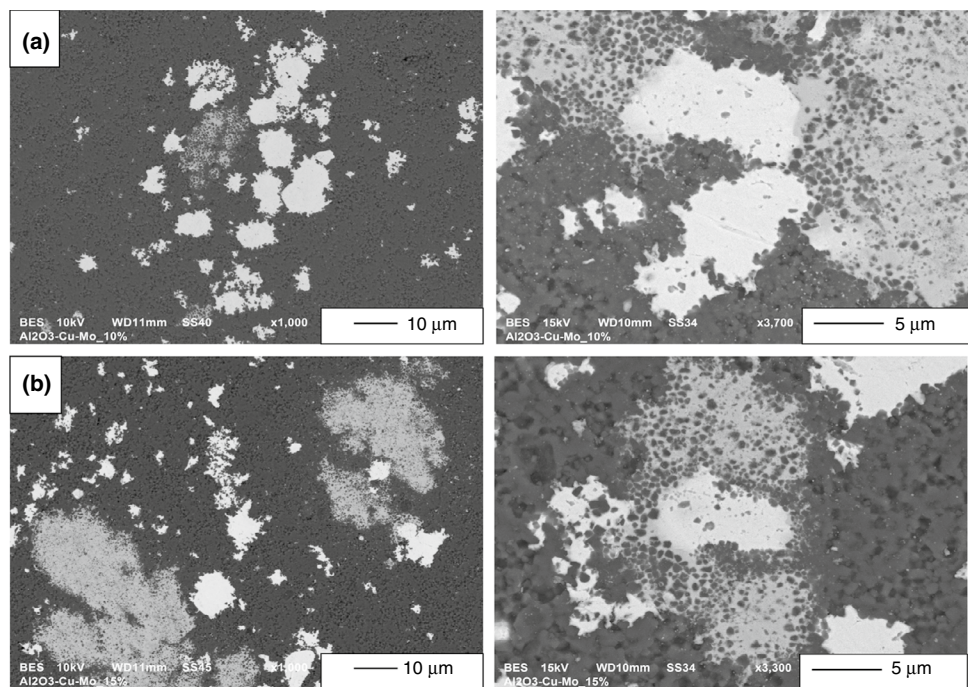
that the copper phase irregularly surrounds around the single particles of molybdenum in both series.

Energy-dispersive X-ray spectroscopy was carried out at three different locations in the samples. Figure 10 shows the concentrations of aluminum, oxygen, copper, and molybdenum from the cross section of composites with 10 vol% of the metal particles (Series I) and with 15 vol% of the metal particles (Series II) after sintering by using EDX investigation. The results of obtained concentration measurements of aluminum, oxygen, copper, and molybdenum for the composites have been collected in Table 4. The observation obtained in this study indicated that analyzed points 1 in both series contain only molybdenum. EDX measurements allowed us to observe that points 2 in fabricated composites with different content of metal content consisted of Al, O, and Cu. In these areas, probably low wettability of ceramics

by molten copper caused the existence of areas consisting of Cu, Al, and O. These areas arise while the flows of molten copper through the pores of the alumina matrix during sintering. Moreover, these points are characterized by different content of chemical elements in all composites, because the flown molten metal probably is not homogenous during sintering. In both series, points 3 contain mainly Al and O, and these areas are corresponding to the ceramic matrix.

The result of the hardness measurements showed that composites from Series I (Al$_2$O$_3$ + 10 vol% metallic phase) were characterized by the hardness value equal to 5.52 ± 0.56 GPa, whereas the hardness of the Series II (Al$_2$O$_3$ + 15 vol% metallic phase) composites was 4.88 ± 0.84 GPa. Compared to the hardness of samples created from pure alumina TM-DAR [26] obtained, the result is lower ca. 11 GPa. This effect may be connected to the

Fig. 10 Analysis of the chemical composition for selected points on the cross section of composite: **a** Series I and **b** Series II
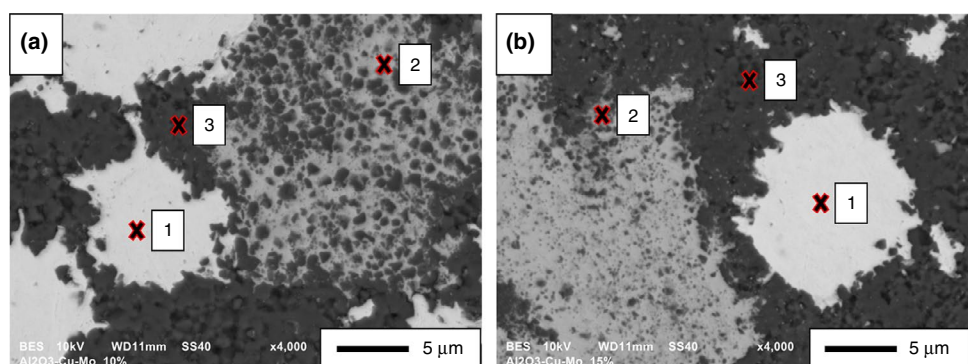
Table 4 Chemical composition of tested composites from different points: (a) Series I—Al_2O_3 + 10 vol% of the metallic phase (Cu + Mo) and (b) Series II—Al_2O_3 + 15 vol% of the metallic phase (Cu + Mo)

| Points	Mass/%			
	Al	O	Cu	Mo
Al_2O_3–Cu–Mo composites				
(a) Series I—Al_2O_3 + 10 vol% metallic phase (Cu + Mo) (Fig. 10a)				
Point 1	–	–	–	100 ± 0.18
Point 2	7.12 ± 0.10	6.89 ± 0.11	85.99 ± 0.14	–
Point 3	56.44 ± 0.17	43.56 ± 0.17	–	–
(b) Series II—Al_2O_3 + 15 vol% metallic phase (Cu + Mo) (Fig. 10b)				
Point 1	–	–	–	100 ± 0.17
Point 2	3.22 ± 0.08	3.52 ± 0.10	93.25 ± 0.12	–
Point 3	54.15 ± 0.16	45.85 ± 0.16	–	–

presence of 10 vol% and 15 vol% metals particles (Cu and Mo) which show plastic deformation that decreases hardness of such composite.

The result of the tensile strength test revealed that the Series I was characterized by a value equal to 79.6 ± 10.7 MPa, whereas the tensile strength for Series II composites was 120.5 ± 9.5 MPa. The experimental results indicate that an increase in the metallic phase content in the composite leads to increased tensile strength. Unfortunately, the results obtained are rather low compared to samples made of pure alumina. International literature reveals that the tensile strength test of sintered Al_2O_3 determined by Brazilian methods should be around 243 MPa for the dynamic test [27, 28]. Based on the obtained results, it can be concluded that the preparation conditions of the composites should be improved to get better properties.

Fractography investigation was performed to reveal the fracture mechanism of the obtained composites. To observe the fracture surfaces, samples after the Brazilian test were used. SEM images in Fig. 11a show the fracture surface of the composite with 10% of metallic phase, while Fig. 11b shows fracture surface of the composite with 15% of metallic phase. Fractography analysis results revealed that in most cases, the bonds between the ceramic matrix and metallic phase are unaffected after the tensile strength test that indicates on good adhesion of matrix and metallic phase. Nevertheless, toughness of the bonds is lower than the toughness of the metallic phases. It can be clarified by the observation of the metallic phases which were not fractured during the test. Fracture observation allowed to conclude that the Al_2O_3 matrix surface is characterized by the brittle fracture mechanism.

Fig. 11 Fracture surface of: **a** Series I—Al_2O_3 + 10 vol% of the metallic phase (Cu + Mo) and **b** Series II—Al_2O_3 + 15 vol% of the metallic phase (Cu + Mo)
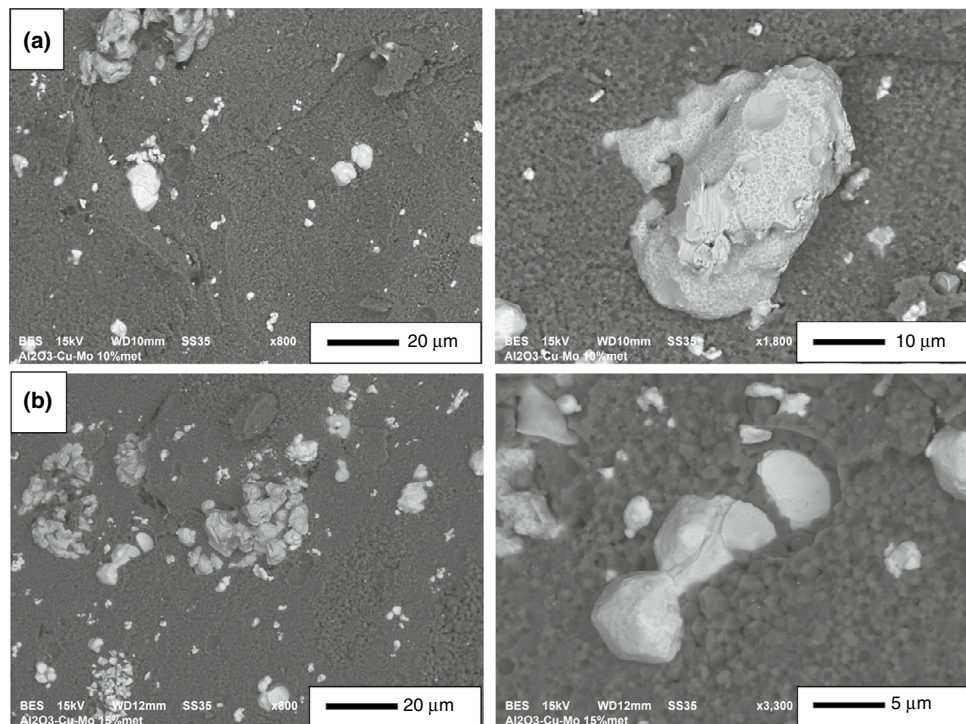
Conclusions

Two series of Al$_2$O$_3$–Cu–Mo composites with different content of metal phases were formed via the slip casting technique.

Based on the present results and discussion, the following conclusions are drawn:

Thermal analysis of Al$_2$O$_3$ composites with different amounts of metallic phase showed subsequent stages of Duramax D3005 decomposition and also mass increasing above the temperature of 600 °C. Mass increasing is connected with Cu and Mo oxidation. Higher content of the metallic phase in the samples causes to higher growth of mass.

Dilatometric experiments showed that an increasing amount of metallic particles into Al$_2$O$_3$ matrix increases the temperature of densification start, increases temperature of maximum densification, and also decreases total shrinkage of the samples during sintering. Metallic particle addition has also an influence on thermal and mechanical properties. The experimental results indicate that an increase in the metallic phase content in the composite leads to increased tensile strength, whereas the hardness decreases with an increasing amount of Cu and Mo particles.

The results of the present investigation indicate that specific heat capacity increased with temperature increasing, while thermal diffusivity decreases with increasing temperature. Specific heat capacity of Al$_2$O$_3$ composites decreased as the amount of metallic phase increases. Carried out research showed that at lower temperatures, the samples without the addition of metallic phase are characterized by the highest diffusivity, whereas the temperature increase leads to an increase in the diffusivity of the samples with the addition of the metallic phase.

The thermal conductivities of Al$_2$O$_3$ composites decreased with an increasing amount of the metallic particles in the structure.

During the sintering, high density composites with Al$_2$O$_3$ as a matrix and copper and molybdenum as a metallic phases were obtained. No new phases between Cu and Mo were revealed independently from the volume content of metallic phase. No homogeneous distribution of the metallic phase was observed. Due to the melting and flowing of the copper during sintering, it irregularly surrounds the single molybdenum particles in both series.

Both hardness and tensile strength of the composite depend on the volume content of metallic phases. Higher content of metallic phase decreases hardness but increases the tensile strength. Lower hardness of the composite with higher metallic phase content is due to lower hardness of Cu and Mo according to alumina. On the other hand, higher tensile strength in samples with higher content of Cu and Mo is a result of good adhesion between ceramic and metal particles what was confirmed by fractography investigation. Higher content of tough ceramic–metal bonds increases the toughness of the composite.

References

1. Gizowska M, Konopka K, Szafran M. Properties of water-based slurries for fabrication of ceramic–metal composites by slip casting method. Arch Metall Mater. 2011;56:1105–10.
2. Chmielewski M, Dutkiewicz J, Kalinski D, Litynska-Dobrzynska L, Pietrzak K, Strojny-Nedza A. Microstructure and properties of hot-pressed molybdenum–alumina composites. Arch Metall Mater. 2012;57:687–93.
3. Qiu J, Dominici JT, Lifland MI, Okazaki K. Composite titanium dental implant fabricated by electro-discharge compaction. Biomaterials. 1997;18:153–60.
4. Bichaud E, Chaix JM, Carry C, Kleitz M, Steil MC. Flash sintering incubation in Al$_2$O$_3$/TZP composites. J Eur Ceram Soc. 2015;35:2587–92.
5. Chen W-H, Lin H-T, Nayak PK, Chang M-P, Huang J-L. Sintering behavior and mechanical properties of WC–Al$_2$O$_3$ composites prepared by spark plasma sintering (SPS). Int J Refract Met Hard Mater. 2015;48:414–7.
6. Garbiec D, Jurczyk M, Levintant-Zayonts N, Mościcki T. Properties of Al–Al$_2$O$_3$ composites synthesized by spark plasma sintering method. Arch Civ Mech Eng. 2015;15:933–9.
7. Dias M, Catarino N, Nunes D, Fortunato E, Nogueira I, Rosinki M, Correia JB, Carvalho PA, Alves E. Helium and deuterium irradiation effects in W–Ta composites produced by pulse plasma compaction. J Nucl Mater. 2017;492:105–12.
8. Travitzki N. Microstructure and mechanical properties of alumina/copper composites fabricated by different infiltration techniques. Mater Lett. 1998;36:114–7.
9. Oh ST, Sekino T, Niihara K. Fabrication and mechanical properties of 5 vol% copper dispersed alumina nanocomposite. J Eur Ceram Soc. 1998;18:31–7.
10. Pietrzak K, Jach K, Kalinski D, Chmielewski M, Morgiel J. Processing and microstructure of Al$_2$O$_3$–Cu composite material interpenetrating network type. In: Proceedings of Euro PM. 2011 Congress and exhibition; 2011. p. 2.
11. Wachowski M, Kaszuwara W, Miazga A, Konopka K, Zygmuntowicz J. The possibility of producing graded Al$_2$O$_3$–Mo,

Al$_2$O$_3$–Cu, Al$_2$O$_3$–W composites using CSC method. Bull Pol Acad Tech. 2019;67:179–84.

12. Khan AA, Labbe JC. Aluminium nitride-molybdenum ceramic matrix composites. Influence of molybdenum addition on electrical, mechanical and thermal properties. J Eur Ceram Soc. 1997;17:1885–90.

13. Zygmuntowicz J, Baczyńska A, Miazga A, Kaszuwara W, Konopka K. Al$_2$O$_3$–Mo functionally graded material obtained via centrifugal slip casting. Ceram Mater. 2017;69:73–7.

14. Nawa M, Sekino T, Niihara K. Fabrication and mechanical behaviour of Al$_2$O$_3$/Mo nanocomposites. J Mater Sci. 1994;29:3185–92.

15. Sbaizero O, Pezzotti G, Nishida T. Fracture energy and R-curve behavior of Al$_2$O$_3$/Mo composites. Acta Mater. 1998;46:681–7.

16. Rohm and Haas. Duramax D-3005 Technical Data Sheet. 2008. https://www.google.com/url?sa=t&source=web&cd=1&ved=2ahUKEwi5x-3SrJPhAhXQo4sKHfzqANQQFjAAegQIABAC&url=http%3A%2F%2Fwww.dow.com%2Fassets%2Fattachments%2Fbusiness%2Fpmat%2Fduramax%2Fduramax_d-3005%2Ftds%2Fduramax_d-3005.pdf&usg=AOvVaw2iFIB42dzWHYkX7L_M2-bh. Accessed 16 July 2019.

17. Tsetsekou A, Agrafiotis Ch, Leon I, Milias A. Optimization of the rheological properties of alumina slurries for ceramic processing applications part II: spray-drying. J Eur Ceram Soc. 2001;21:493–506.

18. Parker W, Jenkins R, Butler C, Abbott G. Flash method of determining thermal diffusivity heat capacity and thermal conductivity. J Appl Phys. 1961;32:1679–84.

19. Oksiuta Z, Perkowski K, Osuchowski M, Zalewska M, Andrzejczuk M. Microstructure and thermal properties of mechanically alloyed W–1%TiC powder consolidated via two-step HIPping. Fusion Eng Des. 2018;126:51–8.

20. ASTM C496/C496M-17. Standard test method for splitting tensile strength of cylindrical concrete specimens. West Conshohocken: ASTM International; 2017.

21. Jiang F, Kulin RM, Vecchio KS. Use of Brazilian disk test to determine properties of metallic–intermetallic laminate composites. JOM. 2010;62:35–40.

22. Scapin ML, Peroni L, Avalle M. Dynamic Brazilian test for mechanical characterization of ceramic ballistic protection. Shock Vib. 2017;2017(2017):1–10.

23. Chmielewski M, Nosewicz S, Kurpaska Ł, Romelczyk B. Evolution of material properties during the sintering process of Cr–Re–Al$_2$O$_3$ composites. Compos Part B Eng. 2016;98:88–96.

24. Chen JJ, Guo BQ, Liu HB, Liu H, Chen P. Dynamic Brazilian test of brittle materials using the split Hopkinson pressure bar and digital image correlation. Strain. 2014;50:563–70.

25. Pietrzak E, Wiecinska P, Pawlikowska E, Szafran M. Colloidal processing of Al$_2$O$_3$ and BST materials. Investigations of thermal stability and decomposition of green bodies. J Therm Anal Calorim. 2017;130:365–76.

26. Zygmuntowicz J, Piątek M, Miazga A, Konopka K, Kaszuwara W. Dilatrometric sintering study and characterization of alumina–nickel composites. Process Appl Ceram. 2018;12:111–7.

27. Yu RC, Ruiz G, Pandolfi A. Numerical investigation on the dynamic behavior of advanced ceramics. Eng Fract Mech. 2004;71:897–911.

28. Tan Y, Yang D, Sheng Y. Study of polycrystalline Al$_2$O$_3$ machining cracks using discrete element method. Int J Mach Tool Manuf. 2008;48:975–82.